Third International Conference on Inverse Design Concepts and Optimization in Engineering Sciences
(ICIDES-III).Editor:G.S.Dulikravich, Washington D.C.,October 23-25,1991

DESIGN OF 3-DIMENSIONAL COMPLEX AIRPLANE CONFIGURATIONS WITH SPECIFIED PRESSURE DISTRIBUTION VIA OPTIMIZATION

Krzysztof Kubrynski
Technical University of Warsaw
Institute of Applied Mechanics
and Aviation Technology
ul. Nowowiejska 24
00-665 Warsaw - POLAND

ABSTRACT: A subcritical panel method applied to flow analysis and aerodynamic design of complex aircraft configurations is presented. The analysis method is based on linearized, compressible, subsonic flow equations and indirect Dirichlet boundary conditions. Quadratic dipol and linear source distribution on flat panels are applied.
In the case of aerodynamic design the geometry which minimizes differences between design and actual pressure distribution is found iteratively using numerical optimization technique. Geometry modifications are modelled by surface transpiration concept. Constraints in respect to resulting geometry can be specified. A number of complex 3-dimensional design examples are presented. The software is adopted to personal computers, and as result an unexpected low cost of computations is obtained.

INTRODUCTION

One of the most important task in aerodynamic design is such airplane shape definition which fulfills the following requirements: low CD, high MA_{DD} and CL_{MAX}, appropriate boundary layer stability and stall progression, elimination of shock waves etc. This, however, depends on appropriate pressure distribution on the surface. It is extremely difficult to fulfill all these requirements for complex, 3-dimensional airplane configurations where strong interference effects occur between aerodynamically close coupled elements. Optimal design of each element does not lead to optimum of configuration because of adverse interference effects. But in principle it is possible to design such configurations with neutral or even favorable interference, where interaction between airplane components gives benefits and leads to better global characteristics then those of separated elements. It is impossible to realize such a configuration only on the ground of experimental technique. Computational methods of aerodynamics, which have developed quickly during last 30 years enable, in connection with the aerodynamic concepts worked out at this time ("roof-top", "peaky" etc.), to realize many interesting designs. The problem can be illustrated by wing-nacelle-pylon configuration. In the past the nacelles were shaped as axisymmetrical body and mounted to swept wing by plane pylons. A strong adverse interference occurs leading to loss in

Third International Conference on Inverse Design Concepts and Optimization in Engineering Sciences (ICIDES-III).Editor:G.S.Dulikravich, Washington D.C.,October 23-25,1991

isobar sweep, higher local Mach numbers and shock waves, losses in lift coefficient at design angle of attack etc., creating the lower aerodynamic efficiency. Later the method of designing for neutral interference was worked out, where nacelle and pylon were shaped along stream lines of isolated wing in order to minimize interference. It is difficult however, even now, to design such configurations with favorable interference.

Slightly simplifying the problem we can consider three kinds of design treatments in aerodynamics using computational methods:

1. Design by trial and error method
2. Direct optimization method
3. Inverse design method

The first is direct transformation of the wind-tunnel technique on the computational ground, where wind-tunnel is replaced by computational system and the process of "aerodynamic model manufacture" and "testing" is significantly cheaper and faster. Experienced aerodynamicist analyses results, specifies the needed modifications and the process is repeated until satisfactory computational results are obtained.

In the second method geometry which minimizes aerodynamic object function (such as drag) and fulfills additional constraints is found directly without external detailed considerations about flow properties. This method, conceptually very attractive and fully automated, can not be actually performed in the case of complex configurations because of very high cost and many times too low accuracy of up-to the date flow analysis methods which lead to so called "numerical noise" and make impossible to find real solution.

The third method is actually the most effective and refined method acceptable in practice. It consists of two steps. First is such a pressure distribution specification which fulfills aerodynamic requirements. In the second step the geometry corresponding to this pressure is calculated using inverse method. It is obvious that the possession of the appropriate inverse method is worthy. The method presented in the paper is actually probably the most general inverse method applied to subsonic flow region, which allows to design of real complex configurations even via interference effects.

FLOW ANALYSIS

The method is based on linearized theory of compressible flow [1].

The Prandtl-Glauert equation

$$\beta^2 \varphi_{xx} + \varphi_{yy} + \varphi_{zz} = 0 \; ; \quad \beta^2 = (1 - Ma_\infty^2) \tag{1}$$

Third International Conference on Inverse Design Concepts and Optimization in Engineering Sciences (ICIDES-III),Editor:G.S.Dulikravich, Washington D.C.,October 23-25,1991

is assumed to govern the perturbation velocity potential in the flowfield. The linearized mass flux boundary conditions on external surface are applied

$$\mathbf{W}\cdot\mathbf{n} = (\mathbf{V}_\infty + \mathbf{w})\cdot\mathbf{n} = \dot{m}_s/\rho_\infty \tag{2}$$

and express the intensity of mass outflow through the surface. $\mathbf{w}$ is the perturbation mass flux vector defined by

$$\mathbf{w} = (\beta^2\varphi_x, \varphi_y, \varphi_z) \tag{3}$$

The second order pressure formula [assuming $\mathbf{V}_\infty = (1,0,0)$]

$$Cp_2 = -2\varphi_x - (\beta^2\varphi_x^2 + \varphi_y^2 + \varphi_z^2) \tag{4}$$

is applied to find aerodynamic forces and moments, and isentropic formula is used to express pressure distribution on the surface:

$$Cp = \frac{2}{kM_\infty^2}\left\{\left[1 + \frac{k-1}{2}M_\infty^2\left[1 - \mathbf{V}.\mathbf{V}\right]^{k/k-1}\right] - 1\right\} \tag{5}$$

Applying Greens Theorem to the flowfield the perturbation velocity potential on the surface can be expressed as:

$$E_P\varphi_P = \frac{1}{4\pi}\iint_{Sb}\left[\frac{-(\dot{m}_s/\rho_\infty - \mathbf{V}_\infty.\mathbf{n}_Q)}{r_\beta} + \varphi_Q\beta^2\frac{\mathbf{r}_{QP}.\mathbf{n}_Q}{r_\beta^3}\right]dS_Q + \frac{1}{4\pi}\iint_{Sw}\langle\varphi\rangle_Q\beta^2\frac{\mathbf{r}_{QP}.\mathbf{n}_Q}{r_\beta^3}dS_Q \tag{6}$$

where $\langle\varphi\rangle$ is the jump of potential across the wake and E is function of position (respectively: 1, 1/2 and 0 for P in the flowfield, on the surface and outside the flowfield). Equation (6) is solved by panel method based on quadratic dipol and linear source distribution on flat panels and indirect Dirichlet boundary conditions (zero perturbation potential is specified on the internal side of surface). Control points and unknown singularity parameters are located in panel center of gravity. Jump of potential across the wake is determined by Kutta condition: flow behind the trailing edge of lifting surface must be tangent to trailing edge bisector. Finally the integral equation (6) is replaced by system of linear equations of the form:

$$[A]\left\{\begin{matrix}\varphi\\---\\\langle\varphi\rangle\end{matrix}\right\} = -\left\{\begin{matrix}0\\-----\\V\infty\circ N_K\end{matrix}\right\} - [B]\left\{\dot{m}_s/\rho_\infty - \mathbf{V}_\infty.\mathbf{n}_Q\right\} \tag{7}$$

Third International Conference on Inverse Design Concepts and Optimization in Engineering Sciences
(ICIDES-III),Editor:G.S.Dulikravich, Washington D.C.,October 23-25,1991

which is solved to obtain the perturbation potential on the surface and jump of potential across the wake. Velocity distribution on the surface is obtained by numerical differentiation of perturbation potential and adding the free-stream contribution. In the local panel coordinate system:

$$\begin{aligned} V_t &= \partial\varphi/\partial t + \mathbf{V}_\infty.\mathbf{t} \\ V_s &= \partial\varphi/\partial s + \mathbf{V}_\infty.\mathbf{s} \end{aligned} \tag{8}$$

INVERSE METHOD

The inverse problem is solved in the present method via optimization. The method is extension of the previous design method of the author. The requested geometry of configuration is searched in a form of sum of the initial geometry and linear combination of basic design shapes:

$$\text{GEOMETRY} = \text{INITIAL GEOMETRY} + \sum_{i=1}^{ND} X_i \circ (\text{i-th BASIC SHAPE}) \tag{9}$$

Coefficients X_i are found from the condition of minimizing the error in pressure distribution:

$$E = \sum_{j=1}^{NP} W_j \circ (Cp_j - Cp_j^D)^2 \tag{10}$$

where: W_j - weight function of j-th point

Cp_j^D - design pressure coefficient

Cp_j - its actual value

using numerical optimization technique.

Direct application of panel method to find the object function brings the high cost of computations. In the presented method the basic design shapes are modelled by surface transpiration. The mass flux through the surface which shift the stream surface with the distance h normal to the initial surface is given by:

$$W_{TR} = \frac{1}{\rho_\infty}\left[\frac{\partial(\rho U h)}{\partial\xi} + \frac{\partial(\rho V h)}{\partial\eta}\right] \tag{11}$$

The mean value of the transpiration over the panel is obtained by mass flux balance in the volume enclosed by body surface and modelled stream surface.

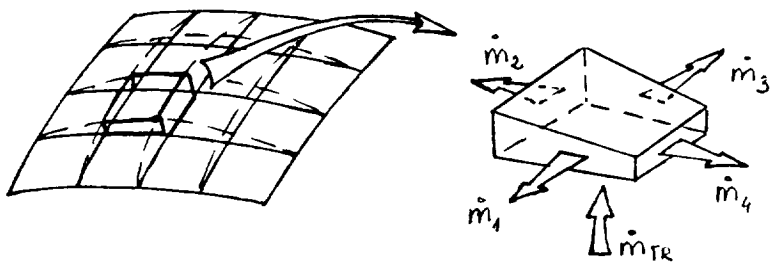

Fig. 1 Mass balance over panel area

The incremental potential distribution due to surface transpiration (i-th basic shape) is calculated from linear equations system similar to (7):

$$\left[A\right]\left\{\begin{matrix}\delta\varphi \\ --- \\ \delta\langle\varphi\rangle\end{matrix}\right\}_i = -\left[B\right]\left\{W_{TR}\right\}_i \qquad (12)$$

Potential on the new geometry is expressed as the sum of initial potential distribution and linear combination of incremental potential distribution due to basic shapes. The new velocity distribution is calculated using eq. (7) with new potential value and unit tangent vectors taken from the new geometry. Geometry redefinition is performed directly using eq. (9). The optimization is performed by quadratic programing method. Additionally geometrical constraints are introduced via penalty function. Gradient and Hessian of object and penalty functions are calculated analytically which lead to high accuracy and low cost. Because of nonlinear nature of the design problem it is solved iteratively using geometry obtained after actual design iteration as initial in the next one. Block diagram of the method is shown on the Fig. 2.

COMPUTER CODE

The method described above was coded in FORTRAN 77 language and implemented on PC-Computers. Because of hardware limitations it is performed as a package of programs. All basic parts of the method are performed by separate computer program, which are sequentially started from batch file. The software package consists of 13 programs including two methods of solution of linear equations system (iterative and block Crout decomposition) and post-processing program. The iterative method of solution performs matrix modification and makes possible to use this method even when other iterative methods do not provide the convergence.
It is possible to use up to 1200 body panels, 500 wake panels, 80 Kutta points, 1280 unknown singularity parameters (plus symmetry condition), and

Third International Conference on Inverse Design Concepts and Optimization in Engineering Sciences (ICIDES-III).Editor:G.S.Dulikravich, Washington D.C.,October 23-25,1991

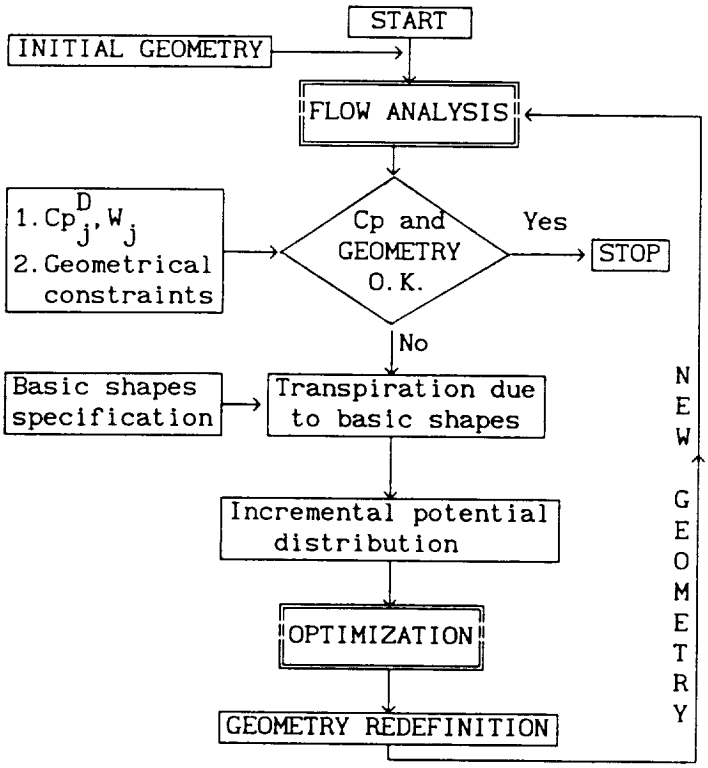

Fig.2 Block diagram of the design method

63 basic design shapes. Flow analysis for PC-386/25MHz and 1000 panels (plus symmetry) took about 25'-40' if using iterative method of solution and about 60' if Crout decomposition method is used. Design process took about 12' for 40 basic design shapes using Crout method. Using computer 486 computing time is about 50% shorter. Cost of such computations is unexpectedly low.

RESULTS

Flow analysis. To show efficiency and accuracy of the method results of analysis of test cases from AGARD AG-241 are shown on Fig. 4 and 5. Results for RAE WING and STRAKED WING with NACA 0002 profile is compared with Datum Results of Rubbert and Roberts.
560 panels were used (40x14) for RAE WING and 640 (40x16) for STRAKED WING. Computing time on PC-386/25MHz respectively 10' (iter)/16.5' (Crout) and 14'/23'. It is seen excellent agreement with compared methods.

Full aircraft configuration design. It consists of wing, body, tail and rear mounted nacelle and pylon. The geometry of the configuration is shown on Fig.6. A new pressure distribution (of "roof-top" type) is specified on the wing upper surface. At all points of pylon where initial negative pressure exceeds Cp = -0.5 this value was specified as design one.

38 basic design shapes of spline-support type were specified. The idea of this type of shapes is shown on Fig. 3. Node lines on the surface in both directions are specified and movement of the node of such network in specified direction corresponds to the desired shape function. To find movement of other points of the surface the interpolation spline is used. The shape functions used correspond to:

-changes of upper surface section of the wing at four control stations (wing-body-junction, η = 0.3, 0.5 and 1.0) corresponding to vertical displacement of points with max. laying at 75%, 55%, 40%, 25%, 15%, 9% and 4% of arc length (measured from leading edge to trailing edge)

-changes of wing twist at wing-body-junction, η = 0.5 and 1.0

-changes of fuselage width in the pylon region with max. at four stations

-changes of nacelle width in the pylon region with max. at three stations

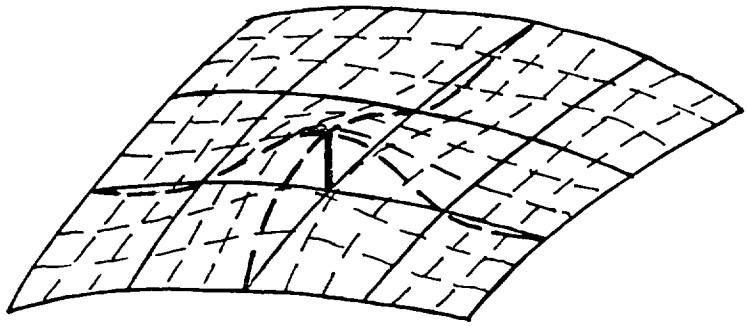

Fig.3 The idea of spline support basic shapes

Geometrical constraints used:

-distance between network points near the trailing edge (for control the trailing angle)

-distance between network points near the max thickness (for control the thickness)

-distance between network points near the leading edge (for control the leading edge radius)

-distance (in vertical direction) between leading edge and trailing edge (for control twist) at three control stations

-distance between points of pylon (at pylon-fuselage intersection) and symmetry plane (for control fuselage shape) at three stations

-distance between points of pylon (at pylon-nacelle intersection) and symmetry plane (for control pylon shape) at three stations.

1042 body panels, 72 wake panels and 1068 unknown singularity parameters for half geometry were used. Computing time using PC-386/25: analysis 78', design cycle 14'. Isobar pattern on the initial geometry and after four design

iterations are shown on Fig.7. Pressure distribution at four wing sections before and after designing are presented on Fig.8 and pressure distribution on the pylon on Fig.9. The shape of body-nacelle region and isobar pattern is shown on Fig. 10. The region of higher negative pressure occurs on the fuselage and nacelle in front of pylon. Adding two shape functions modifying fuselage in front of the pylon and specifying additional points with design pressure, the result (after 4 iterations) as on Fig.11 can be obtained. The convergence history of the design process is shown on Fig.12.

Wing-body-underwing nacelle configuration. The geometry of the configuration and details of nacelle region are shown on Fig.13. 1160 body panels, 104 wake panels and 1183 unknowns were used. The pressure on the wing-body alone configuration was calculated. Results are shown on Fig.14a (lower and upper surface respectively). Pressure distribution obtained for this configuration is used as design pressure for wing-body-nacelle. Adding plane pylon and axisymmetrical nacelle the new pressure distribution and isobar pattern are obtained: Fig.14b. Isobar pattern on the wing after four design iterations is shown on Fig.14c, shape of pylon and nacelle on Fig.15 and pressure at subsequent wing sections before and after designing on Fig.16. Shape of pylon section before and after designing is seen on Fig.17. 38 basic design shapes of spline-support type were used. Wing was changed at three control stations: η = 0.4, 0.5 and 0.6. Four points on upper surface (x/c=0.03, 0.11, 0.27 and 0.50) five points on lower surface (x/c = 0.06, 0.17, 0.33, 0.50 and 0.72) and twist at each of this stations can vary. Additionally four points of upper nacelle contour (x/L = 0.38, 0.50, 0.63 and 0.81) and four points of pylon mean line (x/c = 0.25, 0.50 0.75 and 1.00) were changed. The constraints, in respect to wing thickness and twist, nacelle shape and pylon modification, were specified. It should be noted that despite the constraints used are not very restrictive some of them are active. As result, for example, pylon has nonzero side force (it had tendency to bend more). Convergence history is shown on Fig.18. It is of value to show some aerodynamic coefficient for the configuration:

	Cl_{wing}	$Cl_{nac-pyl}$	Cl_{total}	Cm_{total}
wing-body alone	0.5098	-	0.606	-0.1463
initial	0.4772	0.0051	0.575	-0.1482
designed	0.5096	-0.0008	0.605	-0.1439

Computing time using PC-386/25: flow analysis 84', inverse cycle 15'.

Design of transonic wing. The research wing for jet-trainer type aircraft was designed via subcritical equivalent pressure distribution concept [3] by the author as a part of research investigations on supercritical wing performed at Aviation Institute in Warsaw (unpublished Report of Aviation Institute in Warsaw). The supercritical wing section (of slightly peaky-type pressure distribution) was designed using finite-difference method. Equivalent subcritical pressure distribution for swept wing (sweep angle of leading edge 20.7°, at 25% chord 17.3°) was calculated and used as design pressure on the upper surface of the wing. The originality of the method consist in including the off-design characteristics. By modifying constraints it was forced max. pressure peak at high angle of attack and low Mach number at about η = 0.4, which suggest separation first at this station. If max negative pressure was too high at the station under consideration, the higher leading edge radius was enforced by constraints (worsening, of course, the pressure distribution) and vice versa. 28 basic design shapes were used: five kinds of changes of thickness distribution along the chord at five control stations along the span and twist at three stations. The geometrical constraints in respect to max thickness, trailing edge angle, leading edge radius and twist are utilized.
480 body panels, 24 wake panels and 492 unknown singularity parameters were used. The block diagram of the design process can be introduced as follow:

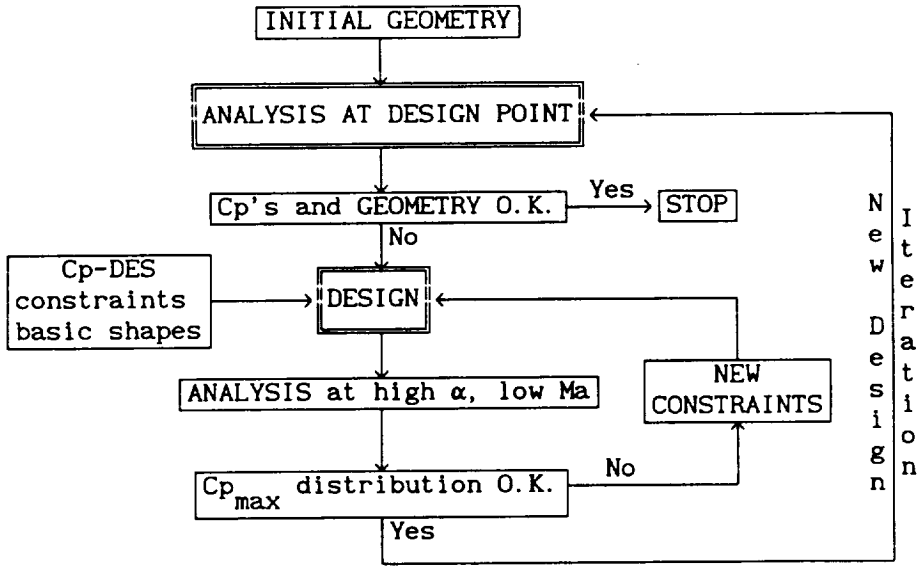

Computing time (386/25): analysis 9' (Crout), 5' (Iter). In each design iteration the flow, at high α, was calculated about 3 times. Resulting isobar

pattern and pressure distribution at three wing sections are presented on Fig.19. Geometrical parameters of the resulting wing are shown on Fig.20. Quite unexpected for swept wing R_{LE} distribution along the span is seen. Max of the leading edge radius occurs at 80% of semispan. Max of pressure peak ($\alpha=12^{\circ}$, Ma=0.2) occurs at η = 0.40. The drag divergence Mach number obtained in wind tunnel tests is shown on Fig.22 and beginning of separation on Fig.23 (unpublished Report of Aviation Institute in Warsaw). It is seen good agreement with expectation.

CONCLUDING REMARKS

The method presented above shows great versatility in the case of design of real, complex configurations. It has nearly no restrictions in respect to the complexity of the geometry. The major limitation is the lack of possibility to take into account modification of planform of the wing and necessity to fix leading edge point (twist can be changed only by moving vertically trailing edge point). It is possible to take into account interference effects in designing, that allows to obtain specified pressure distribution on one element by changing geometry of the other.
Recently the method has been extended to the case of multi-point optimization: the pressure distribution on different parts of the surface can be specified for different angles of attack and the design process is performed at once. The method is exceptionally cheap and efficient because of implementation on PC-computers. The possibility to take into accounts some characteristics at off-design conditions via constrains was shown also.

REFERENCES

1. Ward G.N. - "Linearized Theory of Steady High-Speed Flow" - Cambridge University Press 1955
2. Kubrynski K. - "A Subsonic Panel Method for Design of 3-Dimensional Complex Configurations with Specified Pressure Distribution" - Proceedings of the III GAMM-Seminar in Kiel - Vieweg 1988
3. Slooff J.W. - "Application of Computational Procedures in Aerodynamic Design" - AGARD R-712 1983.

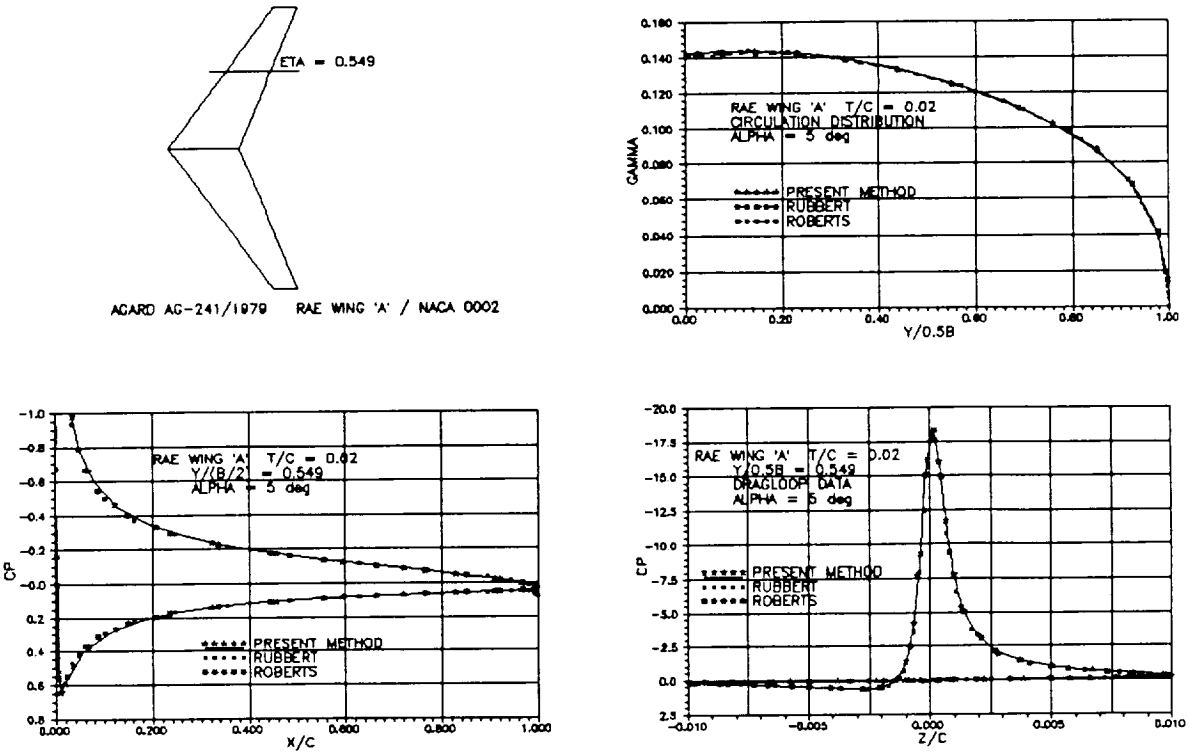

Fig. 4 RAE-WING 'A'/NACA 0002 : comparison of results

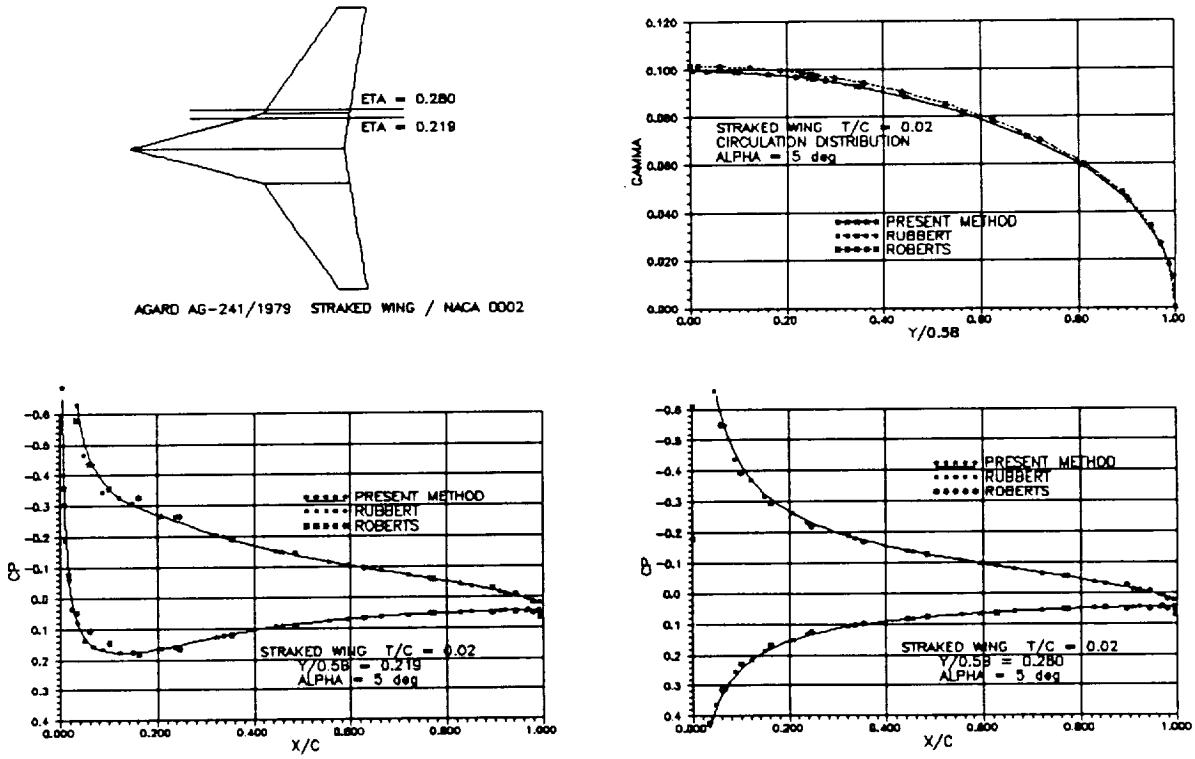

Fig. 5 STRAKED-WING/NACA 0002 : comparison of results

Third International Conference on Inverse Design Concepts and Optimization in Engineering Sciences
(ICIDES-III).Editor:G.S.Dulikravich, Washington D.C.,October 23-25,1991

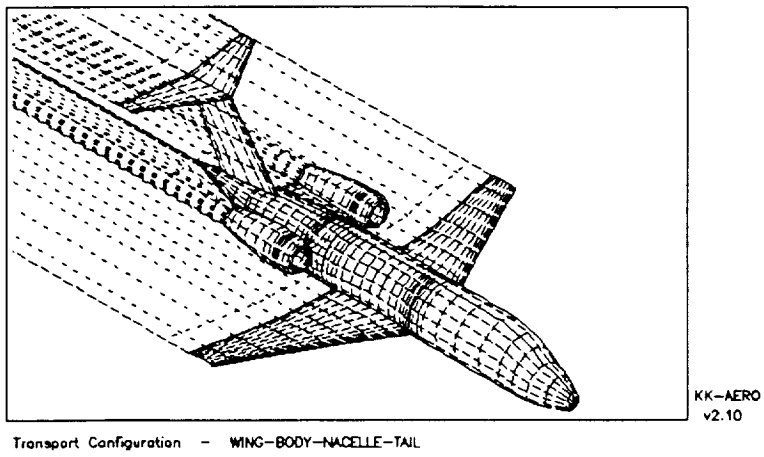

Fig. 6
Network geometry of the entire aircraft configuration

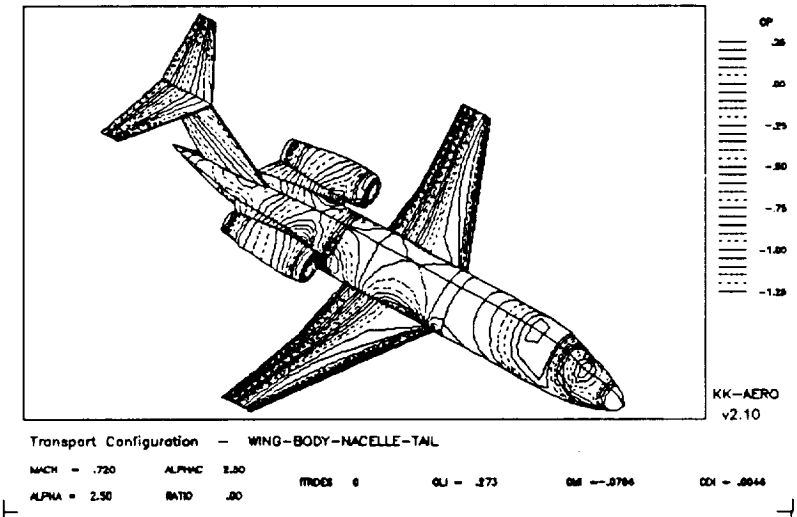

Fig. 7
Isobar pattern on the surface of the initial configuration

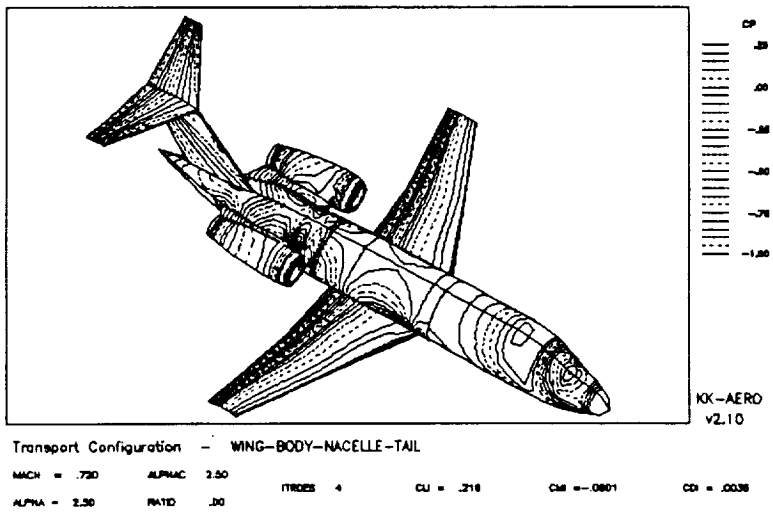

Fig. 8
Isobar pattern on the surface after 4 design iterations

Third International Conference on Inverse Design Concepts and Optimization in Engineering Sciences
(ICIDES-III),Editor:G.S.Dulikravich, Washington D.C.,October 23-25,1991

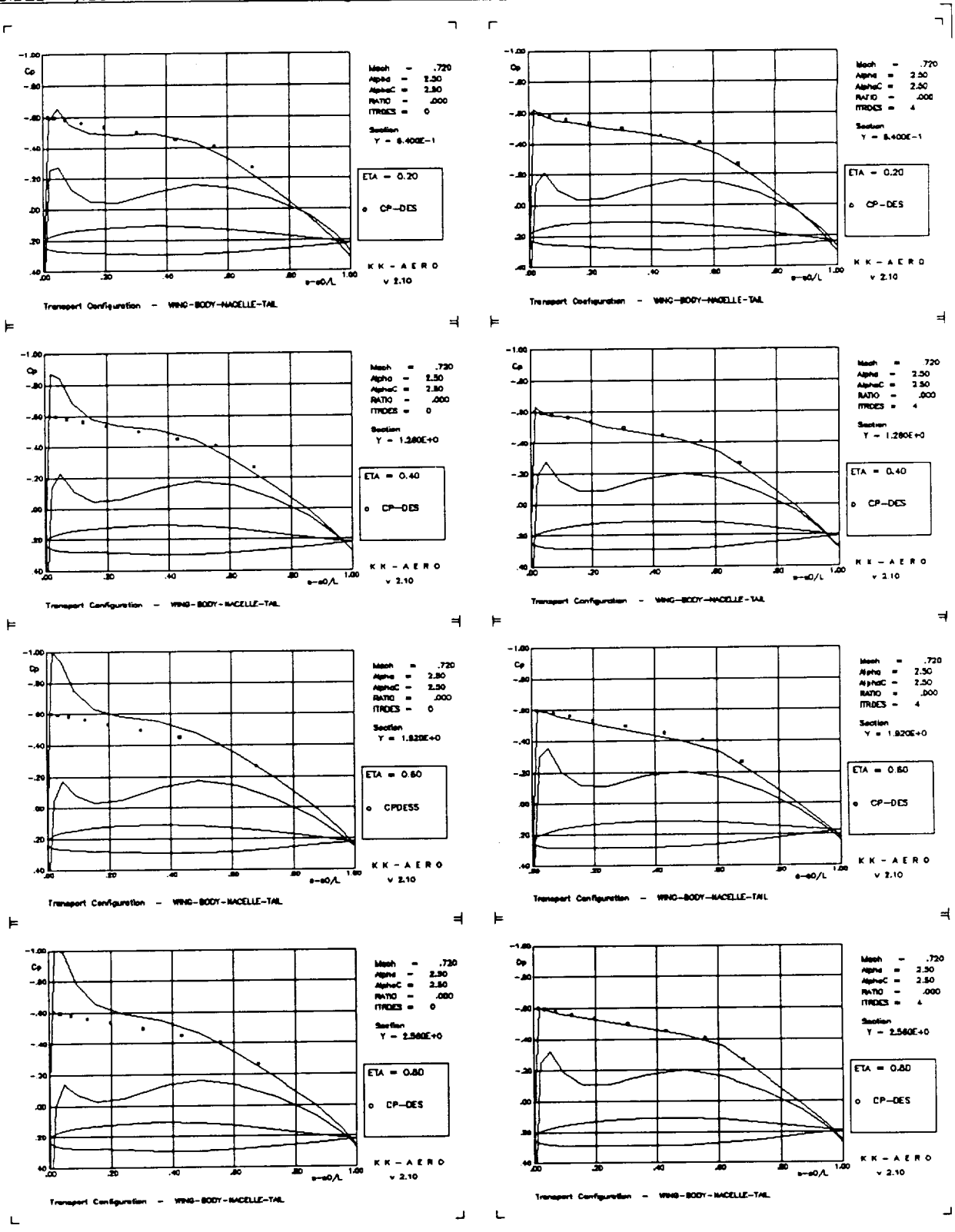

Fig. 8 Pressure distribution on the wing before (left) and after designing (right)

Third International Conference on Inverse Design Concepts and Optimization in Engineering Sciences
(ICIDES-III).Editor:G.S.Dulikravich, Washington D.C.,October 23-25,1991

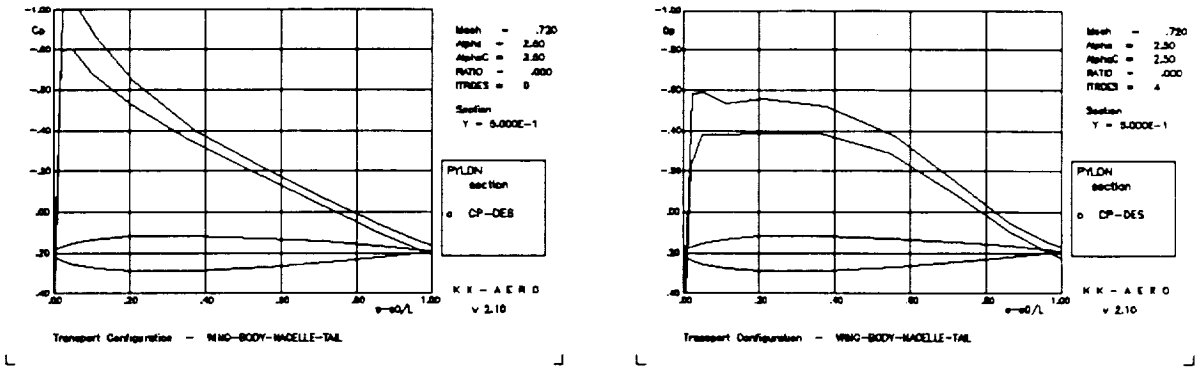

Fig. 9 Pressure distribution on the pylon before and after designing (Cp = −0.5 specified at all points where this value is exceeded)

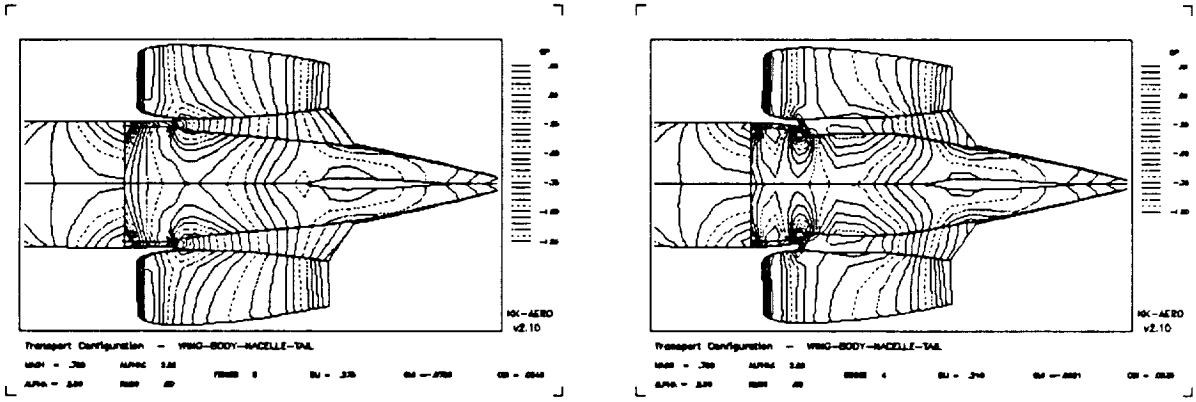

Fig. 10 Fuselage-pylon-nacelle region before and after designing

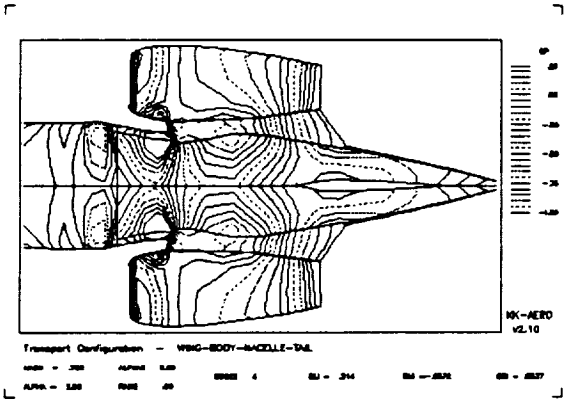

Fig. 11 Fuselage-pylon-nacelle region after designing with additional shape function modyfing fuselage in front of the pylon

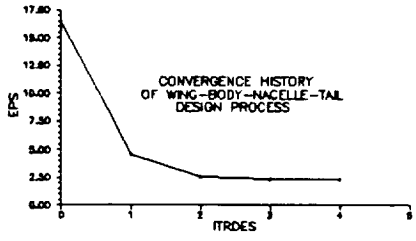

Fig. 12 Convergence of the design process

Third International Conference on Inverse Design Concepts and Optimization in Engineering Sciences
(ICIDES-III),Editor:G.S.Dulikravich, Washington D.C.,October 23-25,1991

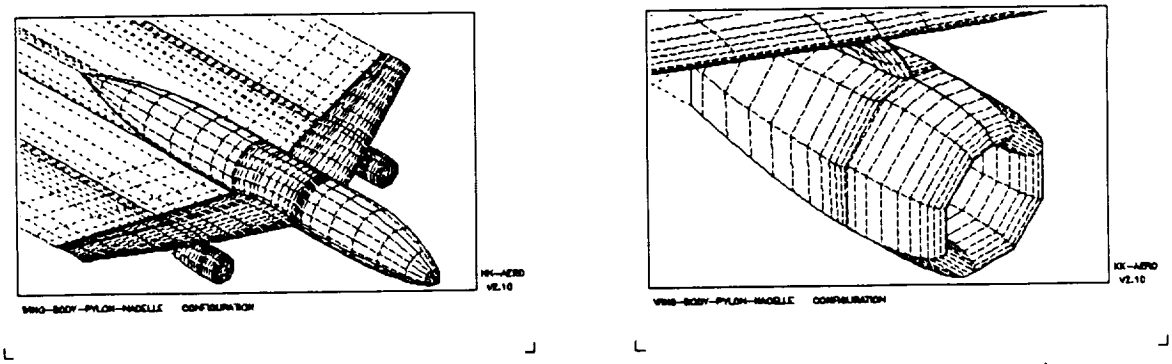

Fig. 13 Geometry of the configuration and details of wing-pylon region

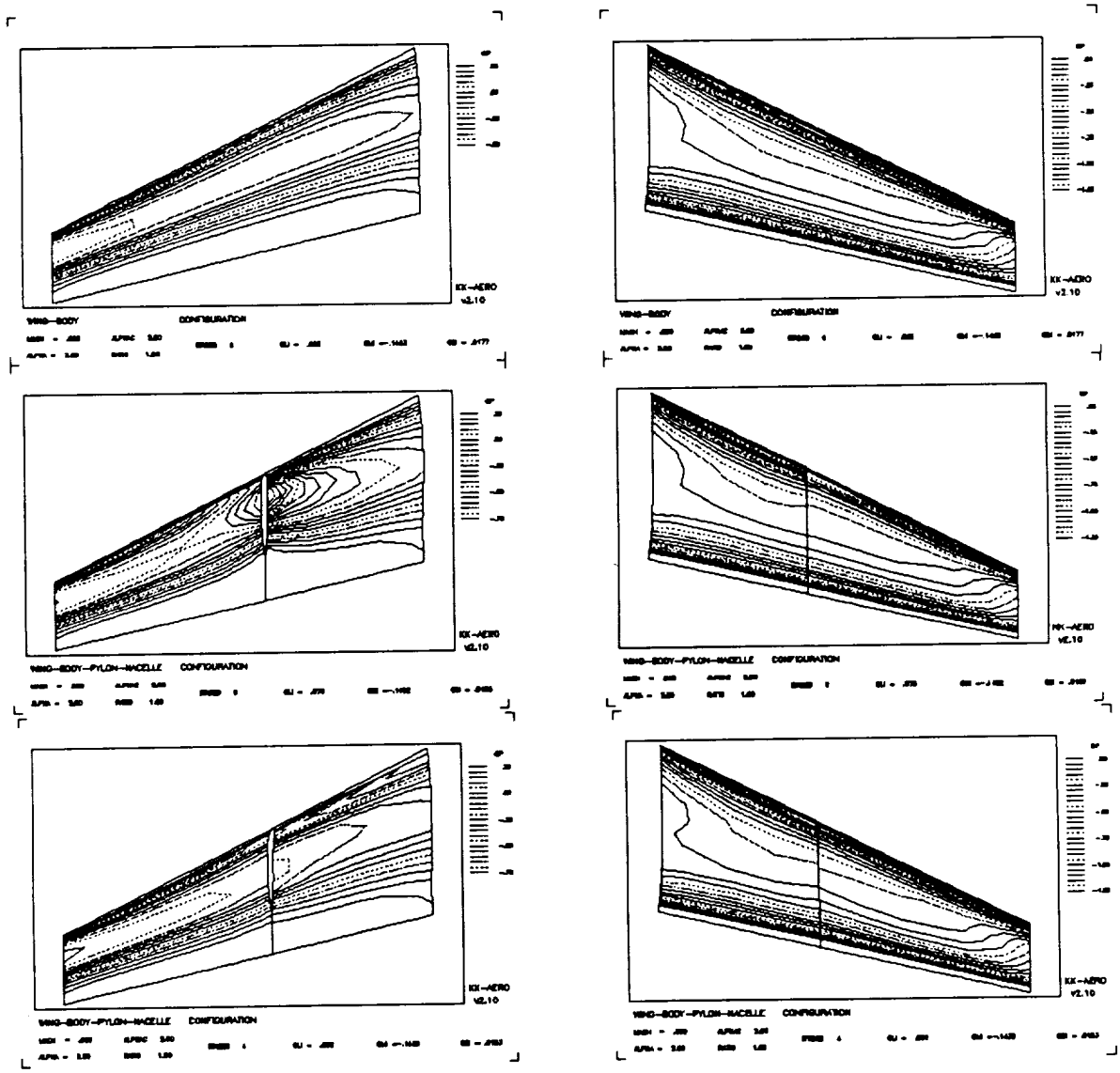

Fig. 14 Isobar pattern on the lower (left) and upper (right) surfaces of the wing: a) without nacelle b) initial geometry c) designed configuration

Third International Conference on Inverse Design Concepts and Optimization in Engineering Sciences (ICIDES-III).Editor:G.S.Dulikravich, Washington D.C.,October 23-25,1991

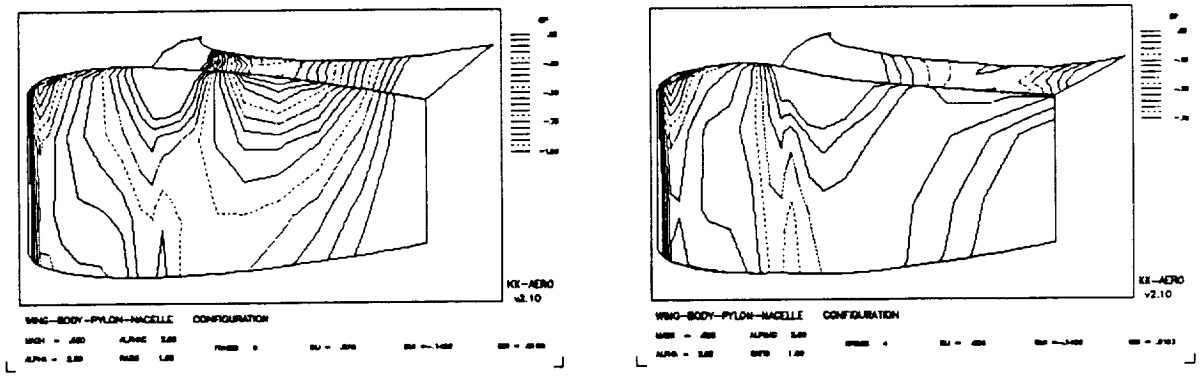

Fig. 15 Contour of the nacelle and pylon before and after design process

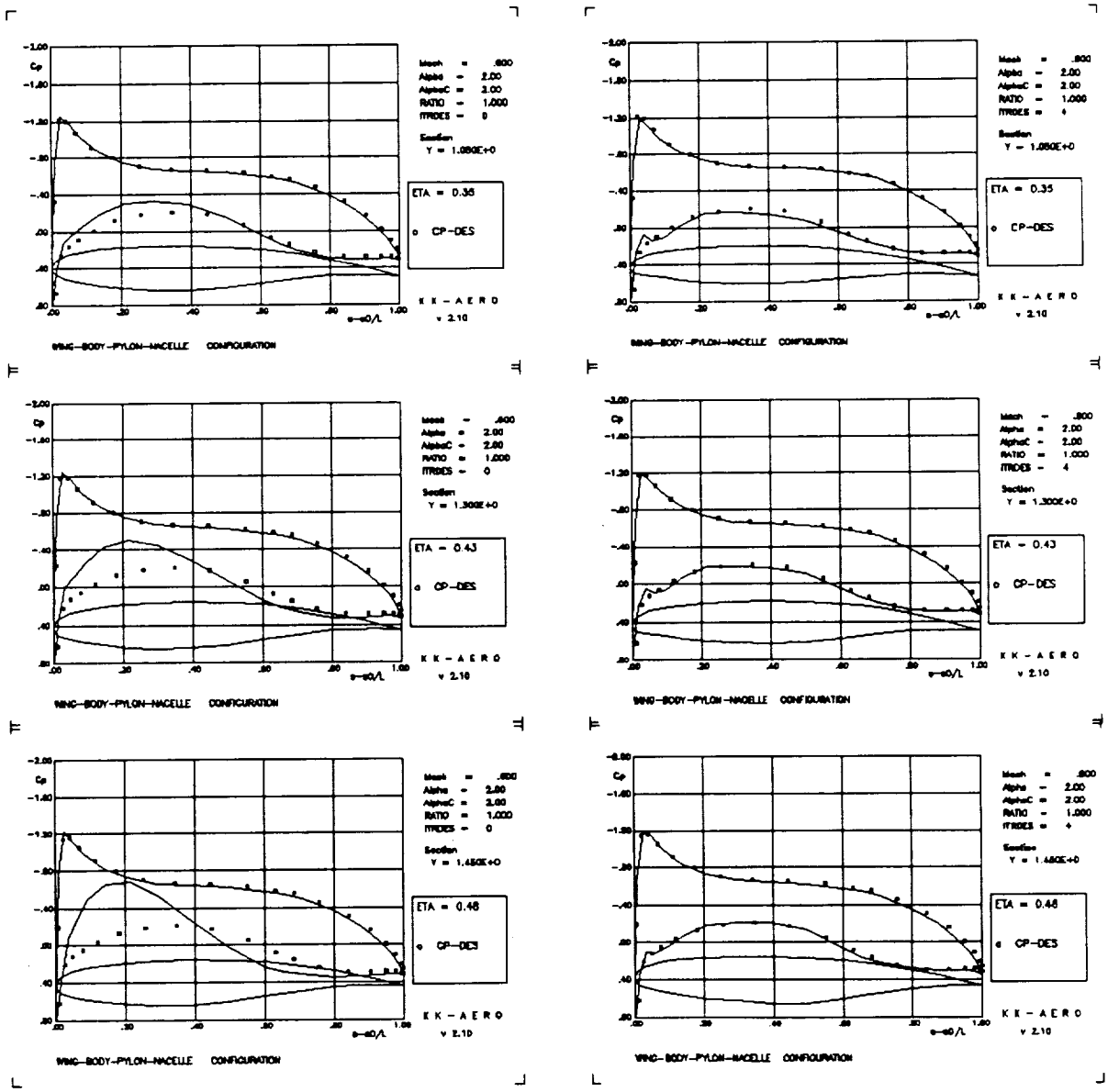

Fig. 16 Pressure distribution on the wing before and after four design iterations

Third International Conference on Inverse Design Concepts and Optimization in Engineering Sciences
(ICIDES-III),Editor:G.S.Dulikravich, Washington D.C.,October 23-25,1991

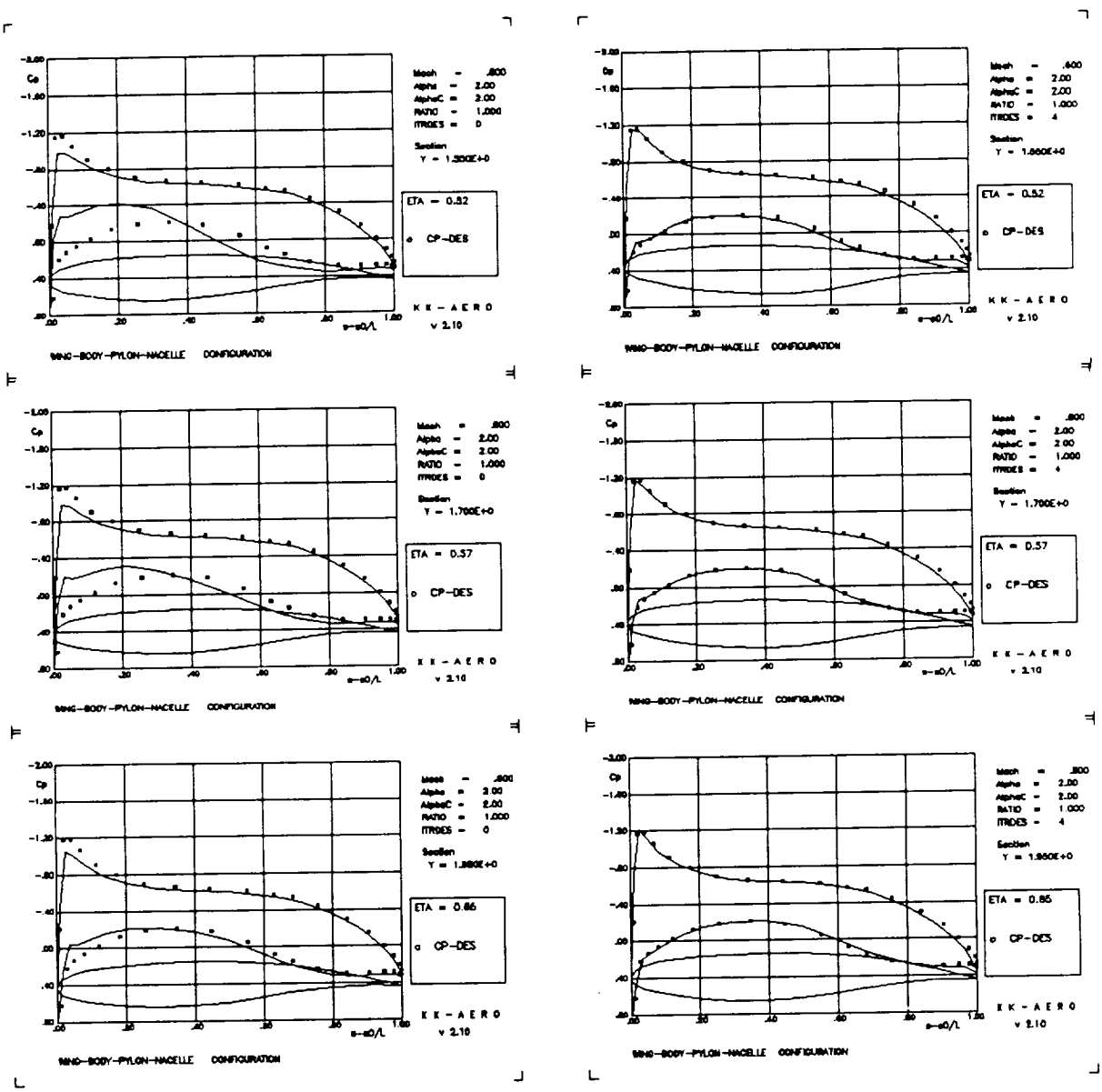

Fig. 16 Pressure distribution on the wing – continued

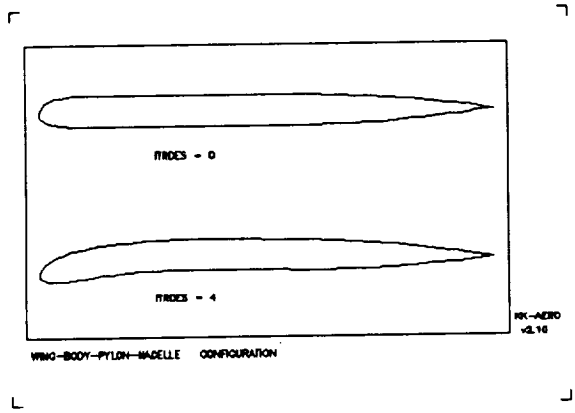

Fig. 17 Cross section of the pylon

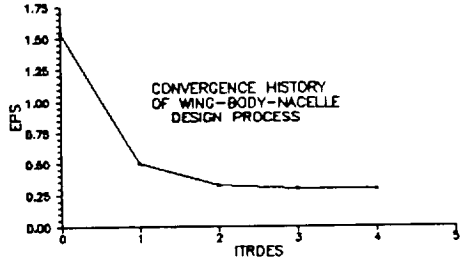

Fig. 18 Convergence of the design process

Third International Conference on Inverse Design Concepts and Optimization in Engineering Sciences
(ICIDES-III),Editor:G.S.Dulikravich, Washington D.C.,October 23-25,1991

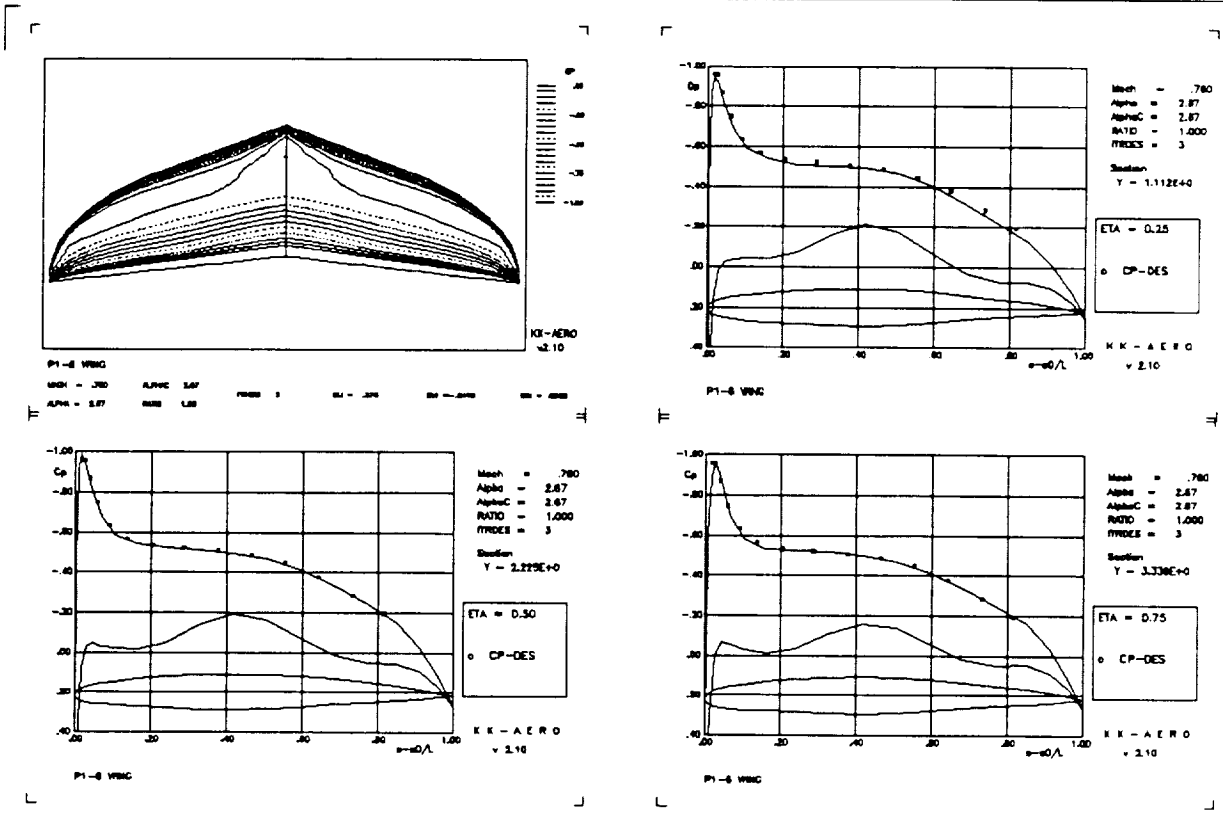

Fig. 19 Planform, isobar pattern and pressure distribution on the designed wing

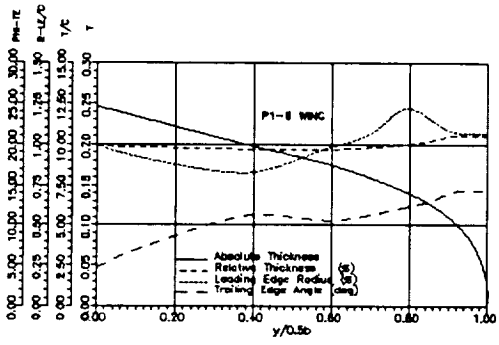

Fig. 20 Geometrical parameters of the designed wing sections

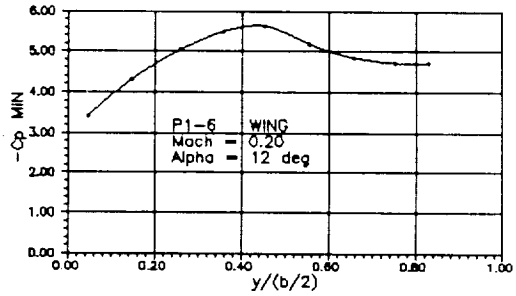

Fig. 21 Peak pressure distribution

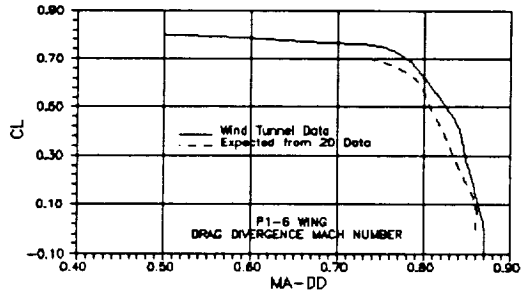

Fig. 22 The drag divergence Mach number

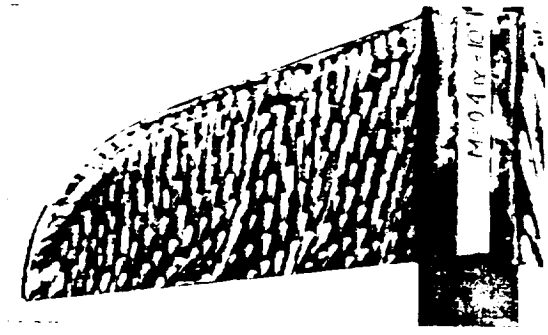

Fig. 23 Begining of separation